Isocyano-triphenylene complexes of gold, copper, silver and platinum. Coordination features and mesomorphic behavior

Rubén Chico,[a] *Cristina Domínguez,* [a,b] *Bertrand Donnio,*[b] *Benoît Heinrich,*[b] *Silverio Coco,**[a] *and Pablo Espinet.**[a]

[a] IU CINQUIMA/Química Inorgánica, Facultad de Ciencias, Universidad de Valladolid, 47071 Valladolid, Castilla y León, Spain. [b] Institut de Physique et Chimie des Matériaux de Strasbourg (IPCMS), UMR 7504 (CNRS-Université de Strasbourg), F-67034 Strasbourg Cedex 2, France.

Stable organometallic complexes [AuX(**CN-TriPh**)] [X = Cl, C_6F_5, C_6F_4O-$C_{10}H_{21}$), C_6F_4O-(*R*)-2-octyl)], **[**(μ-4,4'-$C_6F_4C_6F_4$){Au(**CN-TriPh**)}$_2$], [AuX(**CN-TriPh**)], [CuCl(**CN-TriPh**)], *trans*-[PtI_2(**CN-TriPh**)$_2$] and [Ag(**CN-TriPh**)$_2$]BF_4, bearing the previously unreported triphenylene-isocyanide ligand 1-isocyano-2,3,6,7,10,11-hexadodecyloxytriphenylene (**CN-TriPh**), have been synthesized. The coordination features of the metal ion determine their thermal behavior. The free isocyanide ligand and all of the monomeric gold derivatives display enantiotropic mesomorphic behavior over a wide range of temperature (from 5 to 220 ºC), while the copper complex, with the same stoichiometry but not isostructural with the gold complexes, melts directly to an isotropic liquid. The bis-isocyanide platinum and silver complexes also melt directly to an isotropic liquid at low temperatures. In this case, the two *trans* coordinated isocyanide ligands, connected by a too short linker, cannot become coplanar, which prevents the formation of a mesogenic structure. On the contrary, in the dinuclear gold complex the two isocyanide *trans* ligands are, due to the long Au-C_6F_4-C_6F_4-Au bridge, sufficiently separated to become coplanar and this complex gives rise to a mesophase. The structures of the mesophases were determined by small-angle X-ray scattering. All materials prepared show a fluorescent emission centered on the triphenylene core.

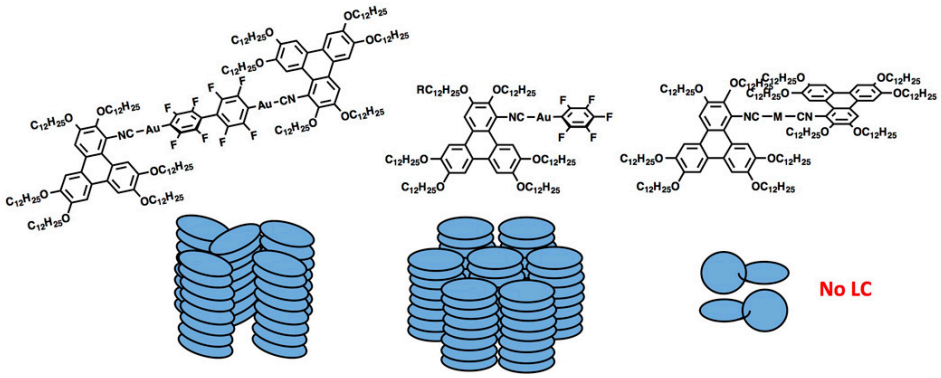

* e-mail: scoco@qi.uva.es; espinet@qi.uva.es

Isocyano-triphenylene complexes of gold, copper, silver and platinum. Coordination features and mesomorphic behavior

Rubén Chico,[a] *Cristina Domínguez,*[a,b] *Bertrand Donnio,*[b] *Benoît Heinrich*,[b] *Silverio Coco,**[a] *and Pablo Espinet.**[a]

[a] IU CINQUIMA/Química Inorgánica, Facultad de Ciencias, Universidad de Valladolid, 47071 Valladolid, Castilla y León, Spain. [b] Institut de Physique et Chimie des Matériaux de Strasbourg (IPCMS), UMR 7504 (CNRS-Université de Strasbourg), 23 rue du Loess, BP 43, F-67034 Strasbourg Cedex 2 (France).

* e-mail: scoco@qi.uva.es; espinet@qi.uva.es

ABSTRACT

Stable organometallic complexes [AuX(**CN-TriPh**)] [X = Cl, C_6F_5, C_6F_4O-$C_{10}H_{21}$), C_6F_4O-(*R*)-2-octyl)], **[**(μ-4,4'-$C_6F_4C_6F_4$){Au(**CN-TriPh**)}$_2$], [AuX(**CN-TriPh**)], [CuCl(**CN-TriPh**)], *trans*-[PtI_2(**CN-TriPh**)$_2$] and [Ag(**CN-TriPh**)$_2$]BF_4, bearing the previously unreported triphenylene-isocyanide ligand 1-isocyano-2,3,6,7,10,11-hexadodecyloxytriphenylene (**CN-TriPh**), have been synthesized. The coordination features of the metal ion determine their thermal behavior. The free isocyanide ligand and all of the monomeric gold derivatives display enantiotropic mesomorphic behavior over a wide range of temperature (from 5 to 220 ºC), while the copper complex, with the same stoichiometry but not isostructural with the gold complexes, melts directly to an isotropic liquid. The bis-isocyanide platinum and silver complexes also melt directly to an isotropic liquid at low temperatures. In this case, the two *trans* coordinated isocyanide ligands, connected by a too short linker, cannot become coplanar, which prevents the formation of a mesogenic structure. On the contrary, in the dinuclear gold complex the two isocyanide *trans* ligands are, due to the long Au-C_6F_4-C_6F_4-Au bridge, sufficiently separated to become coplanar and this complex gives rise to a mesophase. The structures of the mesophases were determined by small-angle X-ray scattering. All materials prepared show a fluorescent emission centered on the triphenylene core.

INTRODUCTION

Columnar discotic liquid crystals are functional materials with great potential for application in electronic devices, such as photovoltaic cells, light emitting diodes, or field effect transistors.[1,2,3,4,5,6,7,8] These devices require high charge-carrier mobility for operation, and columnar liquid-crystalline materials displaying high charge-carrier mobility along their columnar stacks are particularly attractive for this purpose.[1,9,10,11,12] The transfer efficiency depends on the nature and intensity of the intermolecular interactions that maintain the molecular stacks order over long ranges in the columnar structure. Understanding the dynamics and microscopic phase behavior of columnar discotics at the molecular scale is not simple, but it is fundamental for a rational design of new systems and devices with the desired functionality.

An extensively studied type of columnar liquid crystals is based on hexasubstituted triphenylenes, where the stacking of the polyaromatic cores provides an efficient structure for charge transport along the columns.[13] In addition, coordination of metal centers to the triphenylene core offers a versatile way to modify the properties of the system.[14,15,16,17] There are a few reports of liquid crystalline metal-organic triphenylene systems with covalently bonded Hg,[18] Cr^{0},[19] Zn^{II},[20] Cu^{II}, Ni^{II},[21] Ag^{I},[22] and Pt^{II} complexes.[23] Exploring the possibility to develop columnar materials in which columns of different natures coexist, we reported recently a family of mesomorphic mono and dinuclear *ortho*-metallated palladium complexes containing a columnar packing of triphenylene moieties that supports an associated stack of metal moieties.[24] We have also prepared some cationic mixed triphenylene-isocyanide *ortho*-platinated benzoquinolate complexes ($[Pt(bzq)(CNC_6H_4\text{-}O\text{-}(CH_2)_6\text{-}TriPh)_2]A$, $A^- = NO_3^-$, BF_4^-, PF_6^-), displaying a columnar mesophase. The supramolecular structure consists of a central column formed by the self-assembly of the organometallic benzoquinolate-platinum fragments, hexagonally surrounded by six columns formed by stacking of the triphenylene groups. The

central column displays Pt···Pt interactions, which are the origin of the enhanced luminescence and are also responsible for the great stabilization of the mesomorphism.[25]

In the complexes mentioned above the isocyanide group is located at the end of one of the alkoxy chains, so that the triphenylene core and the metallic fragments bonded to the isocyanide group are far apart and electronically disconnected. There are also reports where various electron-withdrawing/donating side groups, such as nitro and amino groups,[26,27,28,29] cyano group,[30] halides,[31,32] and alkyl/alkoxy fragments,[33,34] have been covalently bonded directly to the triphenylene core. The change and the redistribution of the electron density across the aromatic skeleton in these systems, and the consequent change of molecular interactions, modifies markedly the range of existence of the mesophases.[28,35,36] An interesting variation of these two kinds of triphenylene systems is to connect the metal fragment to the triphenylene core using a short conjugated linker. The isocyanide group is an efficient linker, and we are reporting here the synthesis of the previously unreported 1-isocyano-2,3,6,7,10,11-hexadodecyloxytriphenylene (**CN-TriPh**) ligand and its stable isocyanide-triphenylene metal complexes with gold(I), copper(I), silver(I) and platinum(II), and verify how the supramolecular structure and the properties of the original organic system change. The coordination and geometrical features of the metal moiety determine the very different mesomorphic behavior of the materials. The copper, silver and platinum complexes melt directly into an isotropic liquid, but the free isocyanide and all their gold derivatives display enantiotropic columnar mesophases over a wide temperature range. All complexes prepared are fluorescent materials.

RESULTS AND DISCUSSION

Synthesis and Characterization

The triphenylene-isocyanide used in this work, **CN-TriPh**, never reported before was prepared from the corresponding nitroderivative[26] in three steps, as described for other phenyl

isocyanides (Scheme 1).[37] The metal complexes were prepared by reaction of **CN-TriPh** with the corresponding metal precursors, as shown in Scheme 1. C, H, N analyses, yields, and relevant IR and NMR characterization data are given in the experimental part (SI).

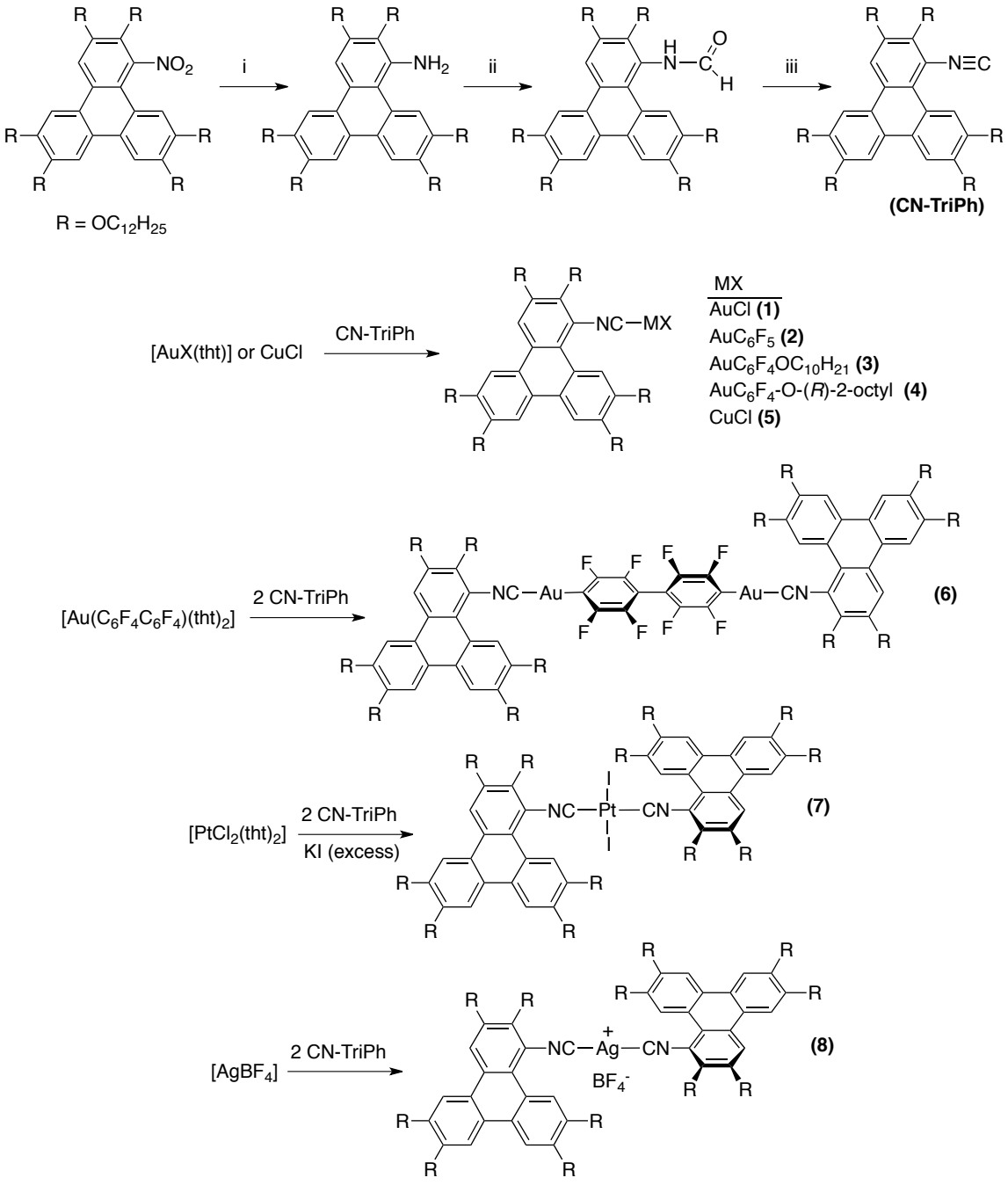

Scheme 1. Synthesis of 1-isocyano-2,3,6,7,10,11-hexadodecyloxytriphenylene (**CN-TriPh**) and the gold(I), **1**-**4**,**6**, copper(I), **5**, silver(I), **8**, and Pt(II), **7**, complexes. i: Sn, CH_3CO_2H; ii: HCO_2H, toluene, reflux; iii: triphosgene, NEt_3, CH_2Cl_2.

The IR spectra of **1-8** show one ν(C≡N) absorption for the isocyanide group. As expected,[38] it appears at higher wavenumbers than in the free ligand **CN-TriPh**, by about 90 cm^{-1} for the Au^{I} complexes, 74 cm^{-1} for the Ag^{I} derivative, 66 cm^{-1} for the Pt^{II} complex and 30 cm^{-1} for the Cu^{I} compound. The observation of one ν(C≡N) IR absorption for **7** supports a *trans* arrangement of the isocyanide ligands.[39]

All the ^{1}H NMR spectra are very similar and display five peaks in the aromatic region, corresponding to the protons situated in the bay positions. The rupture of symmetry produced by incorporation of the isocyanide group and the metallic fragments, makes these protons non-equivalent. The protons of the -OCH_2- fragment appear at 4.2 ppm and the rest of the protons of the alkyl chains in the range 1.94-0.88 ppm.

The ^{19}F NMR spectra of the fluorophenyl complexes show the typical patterns of the corresponding fluorophenyl group: three resonances from an AA'MXX' spin system for the C_6F_5 derivative;[40] two somewhat distorted pseudodoublets from a AA'XX' spin system, with $J_{AA'} \approx J_{XX'}$ for the tetrafluorophenyl complexes;[41] and two complex multiplets at -117.37 ppm and -140.48 ppm, corresponding to the *ortho* and the *meta* fluorine atoms of the two AA'XX' spin systems, for the 4,4'-octafluorobiphenyl compound.[42]

The UV-Vis absorption and fluorescence spectra of the free isocyanide and the metal complexes in dichloromethane solution are summarized in Table 1.

Table 1. UV-Visible and luminescence data for the free isocyanide, and for their metal complexes, in dichloromethane solution at 298 K (10^{-5} M).

Compd.	λ (nm) (ε/10^3 (M^{-1} cm^{-1})	λ_{ex}/nm	λ_{em}/nm	Φ_f (x10^{-3})
(CN-TriPh)	375 (0.1), 320 (23.6), 284 (85.8), 255 (37.1)	283	421	0.2800
(1)	388 (9.7), 337 (22.3), 287 (65.8), 259 (67.4)	280	448	0.0021

(2)	390 (7.4), 337 (18.1), 285 (57.4), 268 (61.6)	283	424	0.0050
(3)	389 (7.6), 337 (18.4), 285 (64.0), 264 (66.6)	280	467	0.0034
(4)	390 (7.2), 337 (17.8), 285 (60.6), 264 (62.0)	281	464	0.0024
(5)	386 (6.6), 335 (19.0), 286 (62.4), 262 (62.0)	285	466	0.1100
(6)	383 (15.4), 329 (34.6), 271 (148.8), 257 (137.9)	282	420	0.0028
(7)	378 (15.1), 329 (41.0), 281 (140.1), 256 (109.4)	280	445	0.0020
(8)	393 (14.8), 332 (29.3), 282 (121.6), 257 (112.8)	284	424	0.0980

The UV-Vis absorption spectrum of the free isocyanide ligand shows a very structured spectral pattern, with typical absorption bands and extinction coefficients (Figure 1) that are assigned as triphenylene π-π* transitions.[43,44] The coordination of the isocyanide to the metal centers produces, in general, wider bands (Figure 1). These changes may arise from the decrease in symmetry and from the loss of planarity induced by the substituents in bay positions, generated upon coordination.[45]

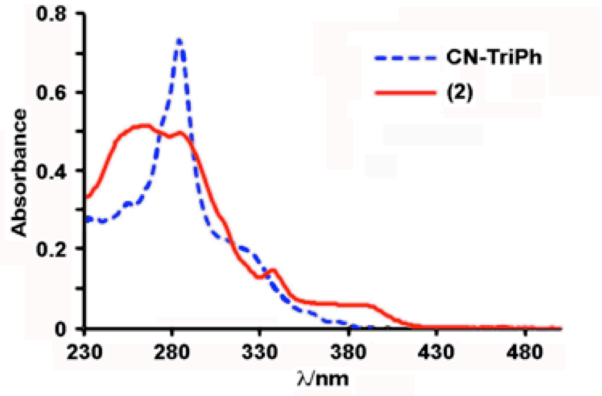

Figure 1. UV-Vis absorption spectra of the free ligand **CN-TriPh** and complex [Au(C_6F_5)(**CN-TriPh**)] **(2)** in dichloromethane (10^{-5} M).

The fluorescence data for the free isocyanide and the metal complexes are listed in Table 3. The free isocyanide and the metal complexes are luminescent at room temperature in dichloromethane solution. As for the electronic spectra, all the emission spectra are similar, with the maximum in the range 421-467 nm (Figure 2), typical of fluorescent 2,3,6,7,10,11-hexaalkoxytriphenylenes.[43,44] The quantum yields for the metal complexes, Φ, measured in dichloromethane solution at room temperature,[46] are considerably lower than for the free isocyanide ligand (Figure 2). It is probable that the presence of the metallic fragment (heavy atom effect) enhances non-radiative deactivation processes. In the solid state, the luminescence of these derivatives is lost, as reported for hexaalkoxytriphenylenes.[43,44]

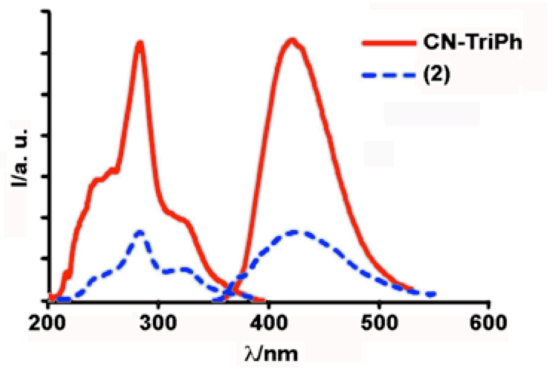

Figure 2. Excitation and emission spectra of the free isocyanide and the complex [Au(C_6F_5)(**CN-TriPh**)] **(2)**.

Thermal behavior and self-organization properties

The mesomorphic properties have been studied by polarized optical microscopy (POM), differential scanning calorimetry (DSC), and small-angle X-ray scattering (SAXS). The optical, thermal and thermodynamic data are gathered in Table 2. In fact, the free isocyanide ligand and all the monomeric gold complexes (**1**-**4**) display enantiotropic mesomorphism over a wide range of temperatures. In contrast the copper complex **5**, with the same stoichiometry, melts directly to an isotropic liquid at 80 ºC, suggesting that this complex is not isostructural with the gold

complexes. The disappearance of the mesomorphic properties presumably originates from the modified geometry: gold ion leads to linear mononuclear derivatives, but copper(I) produces polynuclear complexes $[CuX(CNR)]_n$.[47,48]

The monomeric *trans*-$[PtI_2(\mathbf{CN\text{-}TriPh})_2]$ (**7**) and $[Ag(\mathbf{CN\text{-}TriPh})_2]BF_4$ (**8**) complexes also melt directly to an isotropic liquid at 47-48 ºC. In this case, it is obvious that the two isocyanide ligands, at the separation distance, would collide if they had to become coplanar. For this reason the two discotic fragments have to avoid this spatial conflict and their mean planes arrange twisted relative to each other, loosing the overall discotic shape (Figure 3a,b). In contrast, in the dimeric gold complex (**6**), due to the long Au-C_6F_4-C_6F_4-Au bridge, the two isocyanide *trans* ligands are sufficiently separated to become coplanar and this complex gives rise to a columnar mesophase, and a nematic one at higher temperature (Figure 3c).

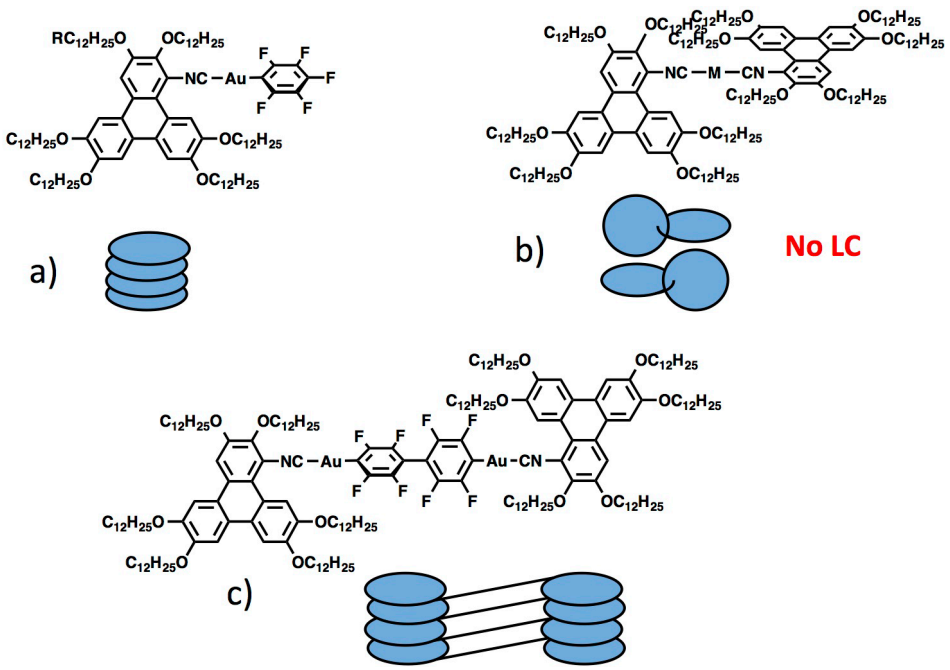

Figure 3. Schematic representation of molecular packing of triphenylene derivatives.

Table 2. Optical, thermal, and thermodynamic data for the free isocyanide and its metal complexes.

Compound	Transition[a]	Temperature[b] (°C)	ΔH[b] (kJmol^{-1})
Isocyanide **(CN-TriPh)**	Cr → Col_{hex} Col_{hex} → I	37 130	58.7 8.6
[AuCl(**CN-TriPh**)] **(1)**	Cr → Col_{hex} Col_{hex} → I	5 220	29.8 10.9
[Au(C_6F_5)(**CN-TriPh**)] **(2)**	Cr → Col_{hex} Col_{hex} → I	7 204	38.2 12.3
[Au(C_6F_4O-$C_{10}H_{21}$)(**CN-TriPh**)] **(3)**	Cr → Col_{hex} Col_{hex} → I	7 206	33.4 9.6
[Au(C_6F_4O-(*R*)-2-octyl)(**CN-TriPh**)] **(4)**	Cr → Col_{hex} Col_{hex} → I	6 207	37.3 13.9
[CuCl(**CN-TriPh**)] **(5)**	Cr → I	80	31.9
[(μ-4,4'-$C_6F_4C_6F_4$){Au(CN-TriPh)}$_2$](6)	Cr → Col_{rec} Col_{rec} → N N → I	102 122 172	7.5 8.9 0.6
trans-[PtI_2(**CN-TriPh**)$_2$] **(7)**	Cr → Cr' Cr → I	30 47	14.1 15.1
[Ag(**CN-TriPh**)$_2$]BF_4 **(8)**	Cr → I	48	47.7

[a] Cr, Cr' crystal phases; Col_{hex}, hexagonal columnar mesophase; Col_{rec}, rectangular columnar mesophase; N, nematic mesophase; I, isotropic liquid;. [b] Data collected from the second heating DSC cycle. The transition temperatures are given as peak onsets. [c] Data from the second heating scan.

As reported for most α-substituted 2,3,6,7,10,11-hexakis(dodecyloxy)triphenylenes,[26,34] a hexagonal columnar phase (Col_{hex}) is generated for 1-isocyano-2,3,6,7,10,11-hexadodecyloxytriphenylene at 37 ºC, and at the remarkably lower temperatures 4-7 ºC for the corresponding mononuclear gold organometallic complexes, [AuX(**CN-TriPh**)] (**1-4**). A Col_{rec} phase at 102 ºC, and a nematic phase at 122 ºC, are observed for the dimetallic compound [(μ-4,4'-$C_6F_4C_6F_4$){Au(**CN-TriPh**)}$_2$] (**6**).

The nematic phase of **6** was identified based on its homogeneous, highly fluid and birefringent optical texture, and by the presence of very mobile line defects and flickering due to fluctuations of the director (Figure 4c,d). The other mesomorphic compounds of the series also exhibit colorful optical textures, and typical features attributed to supramolecular columnar organizations, such as single growing domains (cauliflower heads). Large homeotropic areas further suggest the orthogonal alignment of uniaxial columns. The thermal behavior was fully

reversible and reproducible on subsequent heat/cool cycles. The transition temperatures deduced by POM were in good accordance with those obtained from DSC measurements (Table 2 and Figure 4).

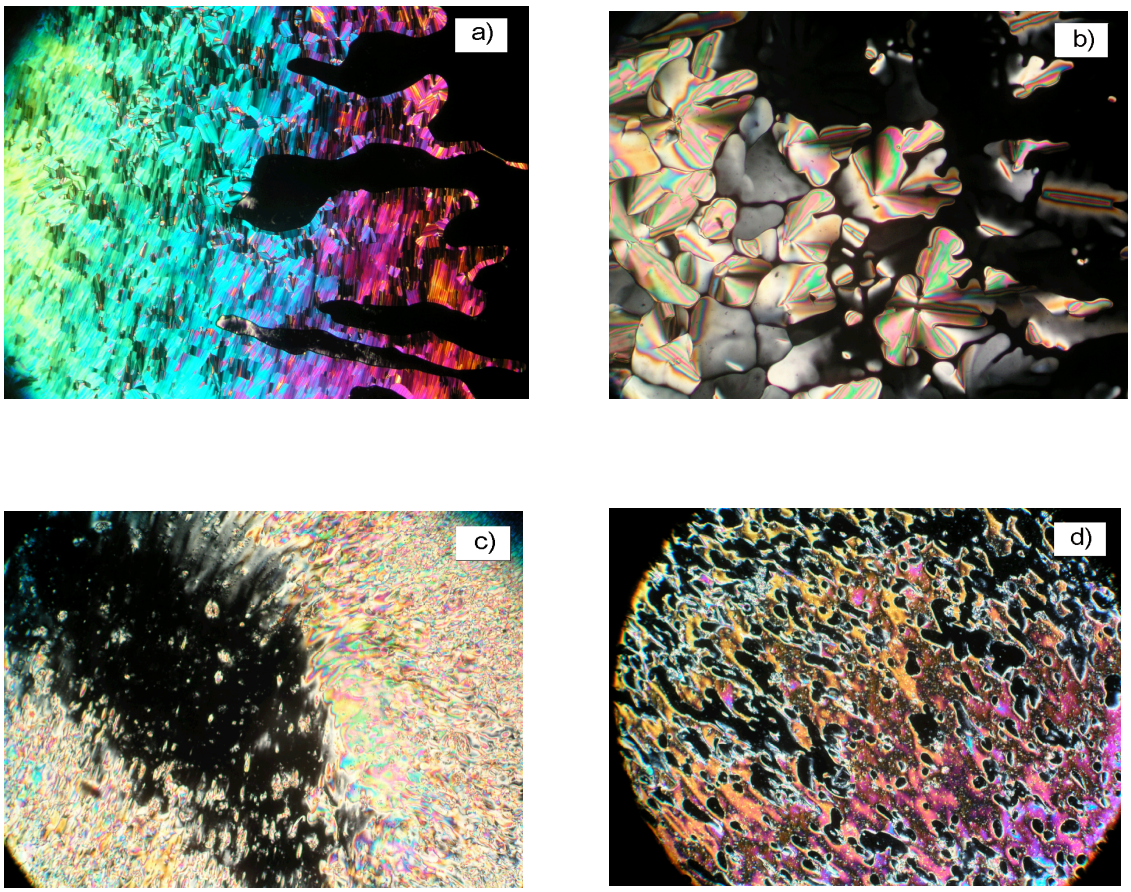

Figure 4. Optical polarising microscopy photographs (x 100) of (a) **CN-TriPh** at 120°C on cooling from the isotropic phase; b) [AuCl(**CN-TriPh**)] at 217°C on cooling from the isotropic phase, c) [(μ-4,4'-$C_6F_4C_6F_4$){Au(**CN-TriPh**)}$_2$]), first heating cycle at 135ºC; d) [(μ-4,4'-$C_6F_4C_6F_4$){Au(**CN-TriPh**)}$_2$]), on cooling at 150ºC. Crossed polarisers.

The presence of the isocyanide group (in the ligand) and the metal-containing fragments (in the complexes) should substantially enhance the electron density of the aromatic skeleton, favoring long-range order stacking and helping to rigidify the columns, leading to stabilization of the mesophase compared to unsubstituted hexakisdodecyloxytriphenylene. Consistently, the isotropization temperature is raised by about 70 °C in the ligand, and complexation further

extends dramatically the mesomorphous temperature ranges (from 93 °C in the ligand to 195-215 °C in the monomeric complexes). The monomeric complexes **1**-**4** preserve the mean cylindrical shape of the columns and the Col_{hex} phase, while the dimeric complex **6** deviates from the purely discotic architecture. The mesomorphism is nevertheless still observed for **6**, but in combination with a symmetry break from hexagonal to rectangular, yielding a Col_{rec} phase. Moreover, the early disappearance of the columnar lattice at around 120 °C is observed, giving rise to a nematic phase, with a range of existence of *ca*. 50 °C, which preserves the common preferential orientation of the columns. Apparently connecting the two-triphenylene units by a rigid bridge intruduces some hindrance to the formation of columns in the mesophase, as previously reported for structurally related triphenylene derivatives.[49] Finally, the gold dimer **6** also shows a shorter liquid crystal range because of its higher melting point (102 ºC) compared to the gold monomers. This higher melting point is related to the contribution of the elongated rigid central part of the molecules to higher cohesion in the crystalline state, as reported for calamitic octafluorobiphenyl liquid crystals.[50,51]

Full identification of the mesophases was attained by small-angle powder X-ray scattering (SAXS) on powder samples measured as a function of temperature from room temperature up to the isotropic liquid. The SAXS profiles of the ligand and the monometallic compounds recorded in the mesophases, reveal from two up to five sharp small-angle peaks of decreasing intensity in the ratio 1:√3:2:√7:3, indexed as the (10), the most intense, (11), (20), (21) and (30) reflections, respectively (Figures 5 and 6, Figures in Supplementary Information), consistent with the packing of supramolecular columns at the nodes of a long-range ordered two-dimensional hexagonal lattice (with one column per lattice as deduced from the molecular volume to lattice cross-section quotient, Table 3). The high intensity of the first order reflection (10) along the abrupt decrease of the intensity of the higher order reflections and harmonics also confirm the

good segregation between the discotic cores including the metal ion with the aliphatic continuum. In the large-angle range, a very strong scattering halo spreading between ca. 3.5 and 5.5 Å (intensity maximum at about 4.4-4.6 Å) was observed, corresponding to the overlapping of different, undifferentiated, lateral distances between the protruding fragments and molten aliphatic tails (h_{fr}+h_{ch}, Table 3), and a relatively sharp and intense signal at larger angle with a maximum at ca. 3.5-3.6 Å, corresponding to the orthogonal stacking of triphenylene cores (h_{π}) correlated over short distances (Figure 5). This correlation length for the intra-columnar packing can be evaluated from the peak thickness at mid height and estimated to lie in the range of ca. 100-150 Å, that is about to 30 to 50 staked molecules. The absence of additional signals associated to the bulky metallic fragments (Figure 6) further suggests that the latter are well confined within the available space between the cavities of the triphenylene cores, without the protruding of the electron-rich gold ion in the aliphatic continuum.[52] This also indicates that the presence of the co-ligands within the aliphatic region (Cl, C_6F_5 and C_6F_4-OR) has only a diluted effect of the electron density redistribution (suggesting that they are randomly distributed around the triphenylene cores, Figure 7). The increase of the bulkiness of the lateral groups, from Cl through C_6F_4OR via C_6F_5, is nevertheless concomitant with the expansion of the lattice dimension and the slight elongation along the column direction, likely due to some local distortions of the aromatic rings, and the enhancement of the aliphatic volume fraction. The molecular volume to lattice cross-section ratio provides a value for h_{mol} of ca 3.45-3.55 Å, depending on the relative size of the lateral group, which is indeed consistent with a 2D arrangement of orthogonally packed columns.

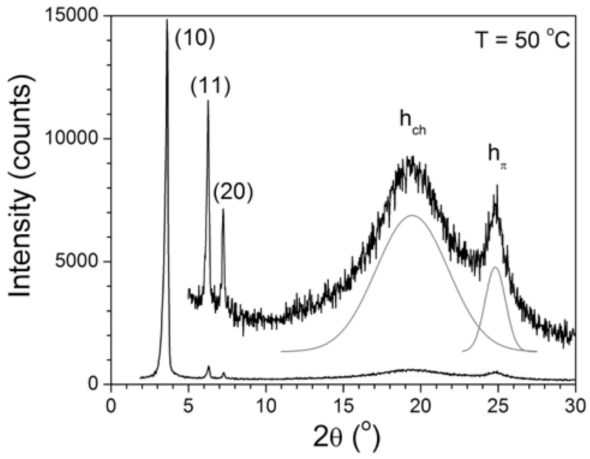

Figure 5. SAXS pattern of **CN-TriPh** recorded in the Col_{hex} phase (T = 50 °C)

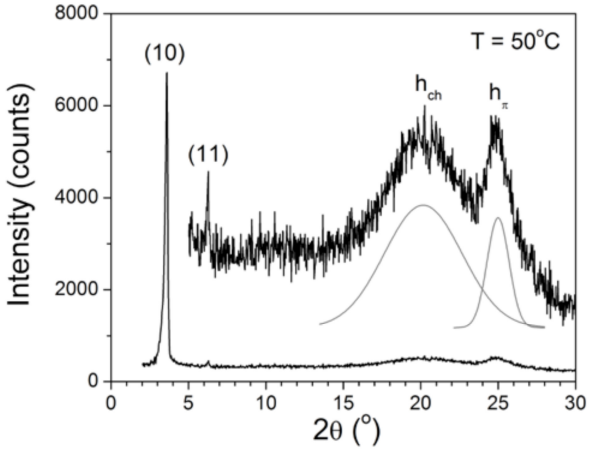

Figure 6. SAXS pattern of [AuCl(**CN-TriPh**)] recorded in the Col_{hex} phase (T = 50 °C).

For the bimetallic compound, the X-ray patterns of the lower temperature phase, recorded between 90 and 120 °C (and down to 70 °C on cooling), and assigned to Col_{rec}, reveals 11 small-angle reflections (Table 2, Figure SI) that could be indexed according to a non-centered rectangular *p*2*gg* lattice. The ratio between the estimated molecular volume versus the area of the cell (Z = 2) provides a value for h_{mol} of *ca*. 3.8 Å, close to $h_{\pi} \approx 3.5$ Å, which is also consistent with a 2D arrangement of nearly orthogonal columns. A detailed analysis of the reflections

further suggests that the phase has a strong lamello-columnar character, particularly on account of the presence of several intense, even lamellar orders (*h*0, *h* = 2*n*) and the concomitant absence of (0*k*) reflections. It can thus be deduced that sub-layers of high electronic density (conjugated aromatic moieties) and aliphatic sub-layers alternate periodically along the *a*-lattice parameter of the rectangular cell, and that the electron density contrast is annihilated along the *b*-parameter by the presence of biphenylene bridges connecting columns of triphenylenes (Figure 7). This rigid connection from the side of the triphenylenes also explains the mesophases broken symmetry with respect to a centered lattice of planar group *c*2*mm*, manifested by the presence of only two reflections of low intensity ((21) and (41); *h*+*k*=2*n*+1).

The interconnection of the columns into continuous lamella leads to the distribution of the bridges on either side of the columns and permits to avoid steric constraints of their largest section (ca 27.5 $Å^2$, i.e. with an average spacing between biphenylenes of ca 5.0 Å). Such a distribution of the bridges seems nevertheless logical and expected as it optimizes the segregation between the various molecular fragments. However, the stacking of the triphenylenes is greatly perturbed by this arrangement, as evidenced by the greatly enlarged and barely visible signal corresponding to the stacking (h_π).

In the nematic phase, formed above 120 ºC, the maximum of the diffuse signal is no longer visible at the position of the h_π signal. However, the asymmetrical profile of the overall low-angle region signal is consistent with the persistence of this band at 3.5-3.7 Å, except that the piles would correlate to a few cycles only, approximately six. Given the structure of the phase below, it is tempting to assign, although not unequivocally, a lamello-nematic type of phase rather than a columnar-nematic one with the sub-layers being decorrelated.

Table 3. Mesophase indexation and parameters.

Compound T/ºC		Indexation			Parameters[d]
	d_{meas}/Å[a]	hk[b]	I[c]	d_{calc}/Å[a]	
CN-TriPh (T = 50 °C, Col_{hex})	24.15 13.94 12.08 4.6 3.45	10 11 20 h_{ch} h_{π}	VS (sh) S (sh) M (sh) VS (br) S (sh)	24.15 13.94 12.07 - -	a = 27.89 Å S = 673 Å^2 ρ = 0.98 g/ cm^3 V_{mol} = 2310 Å^3 N = 1 h_{mol} = 3.43 Å
[AuCl(**CN-TriPh**)] **(1)** (T = 50 °C, Col_{hex})	24.28 14.03 4.4 3.55	10 11 h_{ch}+h_f h_{π}	VS (sh) M (sh) VS (br) S (sh)	24.29 14.02 - -	a = 28.05 Å S = 681 Å^2 ρ = 1.11 g/ cm^3 V_{mol} = 2360 Å^3 N = 1 h_{mol} = 3.47 Å
[AuC_6F_5(**CN-TriPh**)] **(2)** (T = 30 °C, Col_{hex})	25.05 14.48 9.45 4.5 3.6	10 11 21 h_{ch}+h_{fr} h_{π}	VS (sh) M (sh) M (sh) VS (br) S (sh)	25.05 14.46 9.46 - -	a = 28.92 Å S = 725 Å^2 ρ = 1.13 g/ cm^3 V_{mol} = 2535 Å^3 N = 1 h_{mol} = 3.49 Å
[Au$C_6F_4OC_{10}H_{21}$(**CN-TriPh**)] **(3)** (T = 50 °C, Col_{hex})	26.24 15.15 13.04 9.92 8.75 4.5 3.6	10 11 20 21 30 h_{ch}+h_{fr} h_{π}	VS (sh) M (sh) W (sh) W (sh) W (sh) VS (br) S (sh)	26.21 15.13 13.10 9.91 8.74 - -	a = 30.27 Å S = 793 Å^2 ρ = 1.1 g/ cm^3 V_{mol}= 2820 Å^3 N = 1 h_{mol} = 3.55 Å
[Au($C_6F_4OC^*_8H_{17}$)(**CN-TriPh**)] **(4)** (T = 50 °C, Col_{hex})	26.07 15.05 8-10 4.4 3.6	10 11 h_m h_{ch}+h_{fr} h_{π}	VS (sh) W (sh) M (br) VS (br) S (sh)	26.07 15.05 massif - -	a = 30.10 Å S = 785 Å^2 ρ = 1.1 g/ cm^3 V_{mol}= 2780 Å^3 N = 1 h_{mol} = 3.55 Å
[(μ-4,4'-$C_6F_4C_6F_4$){Au(**CN-TriPh**)}$_2$] **(6)** (T = 130 °C, N) (T = 110 °C, Col_{rec})	26.0 4.45 3.7 26.7 23.5 18.9 14.67 13.35 11.96 11.78 9.94 8.88 8.67 7.30	D h_{ch}+h_{mes} h_{π} 20 11 21 31 40 41 22 51 60 13 71 h_{ch}+h_{mes} h_{π}	VS (br) VS (br) M (sbr) VS (sh) VS (sh) W (sh) S (sh) W (sh) W (sh) M (sh) W (sh) W (sh) VW (sh) VW (sh)	- - - 26.68 23.63 18.75 14.75 13.34 11.90 11.82 9.89 8.89 8.67 8.32	a = 53.3 Å b = 26.3 Å S = 1407 Å^2 ρ = 1.05 g/cm^3 V_{mol} = 5345 Å^3 N = 1 h_{mol} = 3.80 Å

	4.45 3.7		VS (br) M (sh)	- -	

Abbreviations: Col_{hex} = hexagonal columnar phase; Col_{rec} = rectangular columnar phase; N = nematic phase. [a]d_{meas} and d_{calc} are the measured and calculated diffraction spacings, respectively (d_{calc} is deduced from the following mathematical expression: $a = 2x\sum[d_{hk}(h^2+k^2+hk)^{1/2}(N_{hk}\sqrt{3})^{-1}]$, where N_{hk} is the number of hk reflections for the Col_{hex} phase and from $d_{hk} = 1/[(h^2/a^2 + k^2/b^2)^{1/2}]$ for the Col_{rec} phase). [b]hk are the Miller indices of the reflections. h_{ch}, $h_{ch}+h_{fr}$, $h_{ch}+h_{mes}$ corresponds to the maximum of the diffuse scattering due to lateral distances between molten aliphatic tails (ch), metallic fragments (fr) and mesogenic bridge (mes); h_{π} corresponds to the stacking periodicity between triphenylene cores. [c]I is the relative intensity of the reflections (VS, very strong; S, strong; M, medium; W, weak; br and sh stand for broad and sharp signal). [d]a is the lattice parameter of the Col_{hex} phase and a and b the lattice parameters of the Col_{rec} phase. Z is the number of columns per lattice, and S is the columnar cross-sectional area ($S = 2a(3)^{-1/2}$ for Col_{hex} , Z = 1, and a×b for Col_{rec}, Z = 2). V_{mol} is the molecular volume and ρ the density, and $h_{mol} = V_{mol}/S$ is the molecular thickness (N=1).

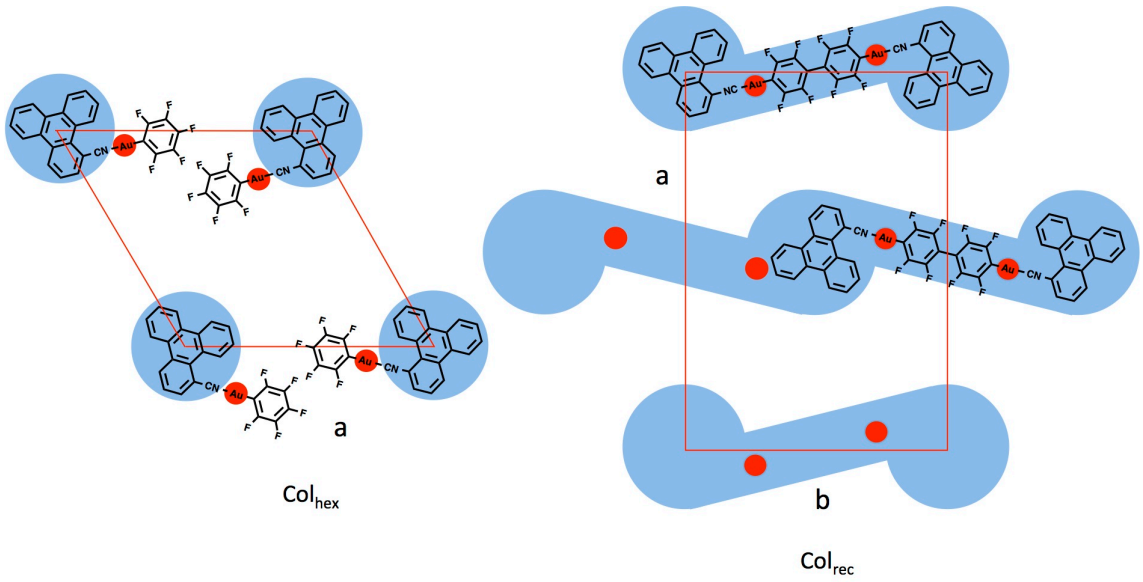

Figure 7. Schematic model of the Col_{hex} and Col_{rec} mesophases formed by the gold complexes (for representative complexes **2** and **6**). For Col_{hex}, random orientation of the side groups around the nodes of the hexagonal lattice preserve the hexagonal symmetry. Aliphatic chains occupying the white zones are not shown for clarity.

CONCLUSIONS

A new prodiscotic isocyanide ligand 1-isocyano-2,3,6,7,10,11-hexadodecyloxytriphenylene (**CN-TriPh**), and a series of metal isocyanide complexes [AuX(**CN-TriPh**)] (X = Cl, fluoroaryle), [(μ-4,4'-$C_6F_4C_6F_4$){Au(**CN-TriPh**)}$_2$], [CuCl(**CN-TriPh**)], *trans*-[PtI_2(**CN-**

TriPh)] and [Ag(**CN-TriPh**)$_2$]BF_4 offer diverse mesomorphism conditioned by the metal fragments. These influence the electronic interactions of the discotic triphenylene moiety, and also the intramolecular availability or restriction to arrange coplanar the triphenylene groups, when more than one is present in the molecule. Again, substituted triphenylene systems provide a powerful and versatile support to metal-containing molecular fragments, enabling to prepare columnar fluid multifunctional materials with metal-containing fragments directly connected to the triphenylene core. All the materials prepared show a fluorescent emission centered on the triphenylene group, which is lost in the solid and the mesomorphic states.

SUPPORTING INFORMATION

Materials and methods. Full details of synthetic methods, spectroscopic data and analytical data for the new compounds. Additional SAXS patterns

ACKNOWLEDGMENTS

This work was sponsored by the Ministerio de Ciencia e Innovación (Project CTQ2014-52796-P) and the Junta de Castilla y León (Project VA302U13). BD and BH thank CNRS and the University of Strasbourg for support.

REFERENCES

[1] Kaafarani, B. R. *Chem. Mater*. **2011**, 378−396.
[2] Pisula, W.; Zorn, M.; Chang, J. C.; Müllen, K.; Zentel, R. *Macromol. Rapid Commun*. **2009**, *30*, 1179−1202.
[3] Kato, T.; Yasuda, T.; Kamikawa, Y. *Chem. Commun.* **2009**, 729−739.
[4] Sergeyev, S.; Pisula, W.; Geerts, Y. H. *Chem. Soc. Rev.* **2007**, *36*, 1902−1929.
[5] Laschat, S.; Baro, A.; Steinke, N.; Giesselmann, F.; Hägele, C.; Scalia, G.; Judele, R.; Kapatsina, E.; Sauer, S.; Schreivogel, A.; Tosoni, M. *Angew. Chem., Int. Ed.* **2007**, *46*, 4832−4887.

[6] Hains, A. W.; Liang, Z.; Woodhouse, M. A.; Gregg, B. A. *Chem. Rev*. **2010**, *110*, 6689−6735.
[7] Oukachmih, M.; Destruel, P.; Seguy, L.; Ablart, G.; Jolinat, P.; Archambeau, S.; Mabiala, M.; Fouet, S.; Bock, H. *Sol. Energy Mater. Sol. Cells* **2005**, *85*, 535−543.
[8] Schmidt-Mende, L.; Fechtenkotter, A.; Müllen, K.; Moons, E.; Friend, R.; MacKenzie, J. *Science* **2001**, *293*, 1119−1122.
[9] Pisula, W.; Kastler, M.; Wasserfallen, D.; Mondeshki, M.; Piris, J.; Schnell, I.; Müllen, K. *Chem. Mater.* **2006**, *18,* 3634−3640.
[10] O'Neill, M.; Kelly, S. M. *Adv. Mater.* **2003**, *15*, 1135−1146;
[11] Kumar, S. *Chem. Soc. Rev.* **2006**, *35*, 83–109.
[12] Wöhrle, T.; Wurzbach, I.; Kirres, J.; Kostidou, A.; Kapernaum, N.; Litterscheidt, J.; Haenle, J. C.; Staffeld, P.; Baro, A.; Giesselmann, F.; Laschat, S. *Chem. Rev.* **2016**, *116*, 1139–1241.
[13] Boden, N.; Bushby, R. J.; Clements, J.; Jesudason, M. V.; Knowles, P. F.; Williams, G. *Chem. Phys. Lett.* **1988**, *152*, 94−99.
[14] Espinet, P.; Esteruelas, M. A.; Oro, L.; Serrano, J. L.; Sola, E. *Coord. Chem. Rev.* **1992**, *117*, 215−274.
[15] *Metallomesogens*; Serrano, J. L., Ed.; VCH: Weinheim, 1996.
[16] Donnio, B.; Guillon, D.; Bruce, D. W.; Deschenaux, R. Metallomesogens. In *Comprehensive Organometallic Chemistry III: From Fundamentals to Applications*; Crabtree, R. H., Mingos, D. M. P., Eds.; Elsevier: Oxford, U.K., 2006; Vol. 12, Chapter.
[17] Bruce, D. W. In Inorganic Materials, 2nd ed.; Bruce, D. W., O'Hare, D., Eds., Wiley: Chichester, 1996; Chapter 8.
[18] Kumar, S.; Varshney, S. K. *Liq. Crystals* **2001**, *28*, 161−163.
[19] Schulte, J. L.; Laschat, S.; Schulte-Ladbeck, R.; von Arnim, V.; Schneider, A.; Finkelmann, H. *J. Organomet. Chem.* **1998**, *552*, 171−176.
[20] Cammidge, A. N.; Gopee, H. *Chem. Comm.* **2002**, 966−967.
[21] Mohr, B.; Wegner, G.; Ohta, K. *Chem. Comm.* **1995**, 995−996.
[22] Yang, F.; Bai, X.; Guo, H.; Li, C. *Tetrahedron Lett.* **2013**, *54*, 409−413.
[23] Shi, J.; Wang, Y.; Xiao, M.; Zhong, P.; Liu, Y.; Tan, H.; Zhu, M.; Zhu, W. *Tetrahedron* **2015**, *71*, 463−469.
[24] Tritto, E.; Chico, R.; Sanz-Enguita, G.; Folcia, C. L.; Ortega, J.; Coco, S.; Espinet, P. *Inorg. Chem.* **2014**, *53*, 3449−3455.
[25] Tritto, E.; Chico, R.; Ortega, J.; Folcia, C. L.; Etxebarria, J.; Coco, S.; Espinet, P. *J. Mater. Chem. C*, **2015**, *3*, 9385−9392.
[26] Boden, N.; Bushby, R. J.; Cammidge, A. N. *Liq. Cryst*. **1995**, *18*, 673-676.
[27] Boden, N.; Bushby, R. J.; Cammidge, A. N.; Headdock, G. *J. Mater. Chem*. **1995**, *5*, 2275-2281.
[28] Kumar, S.; Manickam, M.; Balagurusamy, V. S. K.; Schonherr, H. *Liq. Cryst*. **1999**, *26*, 1455-1456.
[29] Bushby, R. J.; Boden, N.; Kilner, C. A.; Lozman, O. R.; Lu, Z.; Liu, Q.; Thornton-Pett, M. A. *J. Mater. Chem*. **2003**, *13*, 470–474.
[30] Boden, N.; Bushby, R. J.; Lu, Z. B.; Cammidge, A. N. *Liq. Cryst*. **1999**, *26*, 495−499.
[31] Praefcke, K.; Eckert, A.; Blunk, D. *Liq. Cryst*. **1997**, *22*, 113−119.
[32] Boden, N.; Bushby, R. J.; Cammidge, A. N.; Duckworth, S.; Headdock, G. *J. Mater. Chem*. **1997**, *7*, 601−605.

[33] Boden, N.; Bushby, R. J.; Cammidge, A. N.; Headdock, G. *Synthesis*, **1995**, 31−32.
[34] Kumar, S.; Manickam, M.; Varshney, S. K.; Rao, D. S. S.; Prasad, S. K. *J. Mater. Chem*. **2000**, ***10***, 2483−2489.
[35] Destrade, C.; Tinh, N. H.; Gasparoux, H.; Malthete, J.; Levelut, A. M. *Mol. Cryst. Liq. Cryst*. **1981**, *71*, 111−135.
[36] Akopova, O. B.; Kurbatova, E. V.; Gruzdev, M. S. *Russ. J. Gen. Chem.* **2010**, *2*, 268−274.
[37] Cordovilla, C.; Coco, S.; Espinet, P.; Donnio, B. *J. Am. Chem. Soc*. **2010**, *132*, 1424−1431.
[38] Bayón, R.; Coco, S.; Espinet, P. *Chem. Eur. J*. **2005**, *11*, 1079−1085.
[39] Coco, S.; Díez-Expósito, F.; Espinet, P.; Fernaández-Mayordomo, C.; Martín-Álvarez, J. L.; Levelut, A. M. *Chem. Mater.* **1998**, *10*, 3666−3671.
[40] Coco, S.; Espinet, P. *J. Organomet. Chem*. **1994**, *484,* 113−118.
[41] Bayón, R.; Coco, S.; Espinet, P. *Chem. Mater.* **2002**, *14,* 3515−3518.
[42] Coco, S.; Cordovilla, C.; Domíinguez, C.; Espinet, P. *Dalton Trans.* **2008**, 6894−6900.
[43] Markovitsi, D.; Germain, A.; Millié, P.; Lécuyer, P.; Gallos, L. K.; Argyrakis, P.; Bengs, H.; Ringsdorf, H. *J. Phys. Chem.*, **1995**, *99*, 1005−1017.
[44] Marguet, S.; Markovitsi, D.; Millié, P.; Sigal, H.; Kumar, S. *J. Phys. Chem. B* **1998**, *102*, 4697−4710.
[45] Rego, J. A.; Kumar, S.; Ringsdorf, H. *Chem. Mater.* **1996**, *8*, 1402−1409.
[46] Velapoldi, R. A.; Tønnesen, H. H. *Journal of Fluorescence*, **2004**, *14*, 465−472.
[47] Fisher, P. J.; Taylor, N. E.; Harding, M. M. *J. Chem. Soc.* **1960**, 2303−2309.
[48] Bowmaker, G. A.; Hanna, J. V.; Hahn, F. E.; Lipton, A. S.; Oldham, C. E.; Skelton, B. W.; Smith, M. E.; White, A. H. *Dalton Trans*. **2008**, 1710−1720.
[49] Kumar, S.; Varshney, S. K. *Org. Lett.* **2002**, *4*, 157−159.
[50] Coco, S.; Cordovilla, C.; Espinet, P.; Martín-Álvarez, J.; Muñoz, P. *Inorg. Chem.* **2006**, *45*, 10180−10187.
[51] Bayón, R.; Coco, S.; Espinet, P.; Fernández-Mayordomo, C.; Martín-Álvarez, J. M. *Inorg. Chem.* **1997**, *36*, 2329−2334.
[52] Domínguez, C.; Heinrich, B.; Donnio, B.; Coco, S.; Espinet, P. *Chem. Eur. J.* **2013**, *19*, 5988−5995.

FOR TABLE OF CONTENTS USE ONLY.

The coordination features of the metal ion modulate the structures of the fluorescent metal-organic columnar mesophases derived from isocyano-triphenylene ligands.